



SESAM mode-locked Yb:SrLaAlO₄ laser

HUANG-JUN ZENG,¹ ZHANG-LANG LIN,¹ WEN-ZE XUE,¹
GE ZHANG,¹ ZHONGBEN PAN,²  HAIFENG LIN,³ PAVEL LOIKO,^{4,5}
XAVIER MATEOS,^{5,6}  VALENTIN PETROV,⁷  LI WANG,^{7,*}  AND
WEIDONG CHEN^{1,7} 

¹Fujian Institute of Research on the Structure of Matter, Chinese Academy of Sciences, 350002 Fuzhou, China

²Institute of Chemical Materials, China Academy of Engineering Physics, 621900 Mianyang, China

³College of Physics and Optoelectronic Engineering, Shenzhen University, 518118 Shenzhen, China

⁴Centre de Recherche sur les Ions, les Matériaux et la Photonique (CIMAP), UMR 6252 CEA-CNRS-ENSICAEN, Université de Caen Normandie, 6 Boulevard Maréchal Juin, 14050 Caen Cedex 4, France

⁵Universitat Rovira i Virgili (URV), Física i Cristal·lografia de Materials i Nanomaterials (FiCMA-FiCNA), Marcel·li Domingo 1, 43007 Tarragona, Spain

⁶Serra Hünter Fellow, Spain

⁷Max Born Institute for Nonlinear Optics and Short Pulse Spectroscopy, Max-Born-Str. 2a, 12489 Berlin, Germany

*Li.Wang@mbi-berlin.de

Abstract: We report on a detailed investigation of continuous-wave and SESAM mode-locked (ML) laser operation of an Yb:SrLaAlO₄ laser. Pumped with a high-brightness fiber laser at 976 nm, the ML Yb:SrLaAlO₄ laser delivered soliton pulses as short as 38 fs at 1071 nm with an average output power of 86 mW and a pulse repetition rate of ~59 MHz. The maximum average output power reached 1.05 W at 1054 nm for longer pulses (94 fs), corresponding to a peak power of 146 kW and an optical efficiency of 38.6%. To the best of our knowledge, this is the first demonstration of SESAM ML operation of the Yb:SrLaAlO₄ laser.

© 2021 Optica Publishing Group under the terms of the [Optica Open Access Publishing Agreement](#)

1. Introduction

Ytterbium ion (Yb³⁺) doped tetragonal aluminates, e.g., Yb:CaGdAlO₄ (abbreviated Yb:CALGO) and Yb:CaYAlO₄ (abbreviated Yb:CALYO), represent a type of broadband, structurally disordered laser gain media which are extremely suitable for the generation of high-power femtosecond pulses from passively mode-locked (ML) lasers in the spectral region of ~1 μm [1–4]. Yb:CALGO and Yb:CALYO crystals belong to the ABCO₄ crystal family, where A = Ca or Sr, B = Y, Gd, La, etc., and C = Al or Ga. Due to the inhomogeneous spectral broadening originating from their local structure disorder, Yb:CALGO and Yb:CALYO crystals exhibit extremely broad, smooth and flat gain spectral profiles which, combined with attractive thermo-optical properties [5], such as relatively high thermal conductivity and nearly “athermal” behavior, determine their successful applications in the generation of high-average power sub-100 fs soliton pulses at ~1 μm [6–12]. The shortest pulse duration (<30 fs) were achieved via the soft-aperture Kerr-lens mode locking (KLM) technique from Yb:CALGO and Yb:CALYO lasers [13–16].

The success of the Yb:CALGO and Yb:CALYO crystals paves the way to further explore other Yb³⁺-doped disordered aluminate crystals as femtosecond laser gain media. Very recently, we developed a novel Yb³⁺-doped strontium lanthanum aluminate crystals grown by the Czochralski method, i.e., Yb:SrLaAlO₄, abbreviated Yb:SALLO [17]. It is also an ABCD₄-type compound belonging to the tetragonal system with a K₂NiF₄ structure (space group *I4/mmm*). The Yb:SALLO crystal exhibits relatively large absorption bandwidths of 24 nm for π- and 14 nm for σ-polarization (full width half maximum, FWHM). The broadband absorption releases

the requirement of wavelength stabilization for the pump sources and facilitates power scaling by using commercially available high-power InGaAs laser diodes. The lattice disorder in the structure of the Yb:SALLO crystal provides a variation of the local crystal field around the Yb³⁺ dopant ions resulting in a considerable inhomogeneous spectral broadening. As a result, Yb:SALLO exhibits also broad, flat and smooth spectral gain profiles supporting sub-50 fs pulse generation from ML lasers. Recently, we demonstrated the first passively ML operation of an Yb:SALLO laser with soliton pulses as short as 44 fs via soft-aperture KLM technique [18]. Compared to its Yb:CALGO and Yb:CALYO counterparts, Yb:SALLO features: (i) lower melting point ($\sim 1650^\circ\text{C}$) [19], (ii) higher crystallinity and better optical quality and (iii) slightly broader spectra of Yb³⁺ dopant ions. The drawback of SALLO is the lower segregation coefficient for Yb³⁺ ions, $K_{\text{Yb}} = 0.235$ [17].

The promising spectroscopic features, as well as the previous promising ML results motivated us to further explore the potential of Yb:SALLO. Implementing a Semiconductor Saturable Absorber Mirror (SESAM) for starting and stabilizing the soliton pulse generation and dispersive mirrors (DMs) for intracavity group delay dispersion (GDD) management, we demonstrate sub-40 fs soliton pulse generation from a SESAM ML Yb:SALLO laser.

2. Experimental setup

The schematic of the Yb:SALLO laser is shown in Fig. 1. The high quality Yb:SALLO crystal with an Yb³⁺ doping of $1.36 \times 10^{20} \text{ cm}^{-3}$, corresponding to 1.175 at.% was employed. A cubic sample with an aperture of $3 \text{ mm} \times 3 \text{ mm}$ and a thickness of 3 mm was cut for light propagation along the *a*-axis (*a*-cut). This crystal orientation was selected to ensure access to the desirable π -polarization corresponding to stronger pump absorption. The two sides of the crystal were polished to laser quality and remained uncoated.

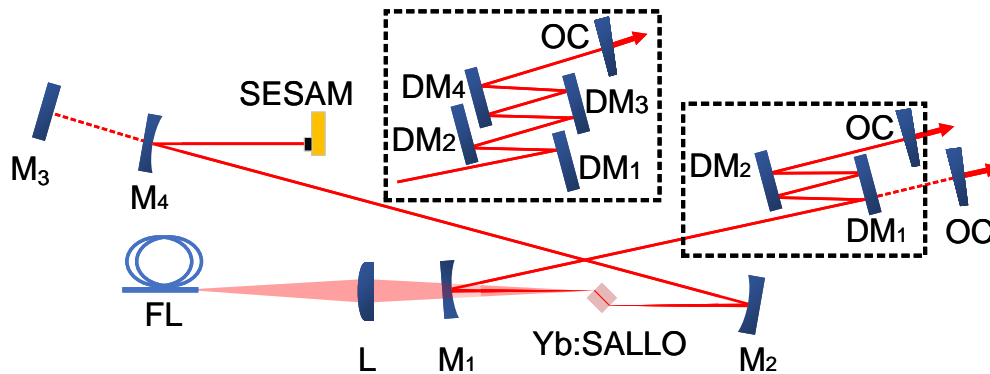


Fig. 1. Schematic of the Yb:SALLO laser. FL: fiber laser; L: spherical focusing lens; M₁, M₂ and M₄: concave mirrors (RoC = -100 mm); M₃: flat rear mirror used in the CW regime; DM₁ - DM₄: flat dispersive mirrors; OC: output coupler; SESAM: SEMiconductor Saturable Absorber Mirror.

An X-folded astigmatically compensated linear cavity was constructed to evaluate the performance of the Yb:SALLO crystal both in the continuous-wave (CW) and ML regimes. The laser crystal was mounted in a water-cooled copper holder (coolant temperature: 20°C) and placed at the Brewster's angle between the two concave mirrors M₁ - M₂ (radius of curvature, RoC = -100 mm) to minimize the insertion loss. The pump source was a CW, narrow-linewidth (50 kHz) fiber laser at 976 nm. It emitted a nearly diffraction-limited beam with a propagation factor (M^2) of ~ 1.03 . The pump beam was focused into the laser crystal through the dichroic mirror M₁ by a

spherical focusing lens with a focal length of 75 mm, which resulted in a beam waist of $16.2 \mu\text{m} \times 29.5 \mu\text{m}$ in the sagittal and tangential planes, respectively.

In the CW regime, a four-mirror cavity was used: one cavity arm was terminated by a flat rear mirror M_3 and another arm – by a flat-wedged output coupler (OC) having a transmission at the laser wavelength T_{OC} in the range 1% - 10%, see Fig. 1. The cavity mode size in the crystal by the ABCD formalism yielded the radii of $24 \mu\text{m} \times 47 \mu\text{m}$ in the sagittal and the tangential planes, respectively.

For ML operation, the mirror M_3 was replaced by a curved mirror M_4 (RoC = -100 mm) to create a second beam waist on the SESAM to ensure its deep bleaching. A commercial SESAM (BATOP, GmbH) with a modulation depth of 1.2%, a relaxation time of ~ 1 ps and a non-saturable loss of $\sim 0.8\%$ was implemented for starting and stabilizing the ML operation. The calculated radius of this second beam waist was $\sim 77 \mu\text{m}$. The intracavity GDD was optimized by inserting two or four different flat dispersive mirrors (DMs) in the other cavity arm having a negative GDD per bounce of: $DM_1 = -250 \text{ fs}^2$, $DM_2 = -250 \text{ fs}^2$, $DM_3 = -100 \text{ fs}^2$ and $DM_4 = -55 \text{ fs}^2$. The group velocity dispersion (GVD) of the Yb:SALLO crystal was estimated from the dispersion curves [20] to be $220 \pm 50 \text{ fs}^2/\text{mm}$ at 1050 nm for π -polarization.

3. Continuous-wave laser operation

The Yb:SALLO laser generated a maximum CW output power of 1.42 W at 1051.6 nm with a high slope efficiency of 67.3% and a low laser threshold of 121 mW (for $T_{OC} = 2.5\%$ and an absorbed pump power of 2.22 W), see Fig. 2(a). The measured single-pass pump absorption under lasing conditions depended on the transmission of the OCs ranging from 25% to 49%, indicating a certain ground-state bleaching being suppressed by the recycling effect. The laser threshold gradually increased with the transmission of the OC, from 66 mW ($T_{OC} = 1\%$) to 285 mW ($T_{OC} = 10\%$). The laser spectra varied with the output coupling: for low T_{OC} of 1%, the laser operated at two lines, 1050 and 1068 nm, for intermediate $T_{OC} = 1.6\% - 2.5\%$ - only at ~ 1051 nm and for high $T_{OC} = 7.5\% - 10\%$ - at yet shorter wavelength of ~ 1016 nm, see Fig. 2(b). Such a blue-shift of the laser wavelength with increasing the output coupling is typical for quasi-three-level Yb^{3+} lasers with inherent reabsorption at the laser wavelength and it agrees with the gain spectra of Yb:SALLO for π -polarization [17].

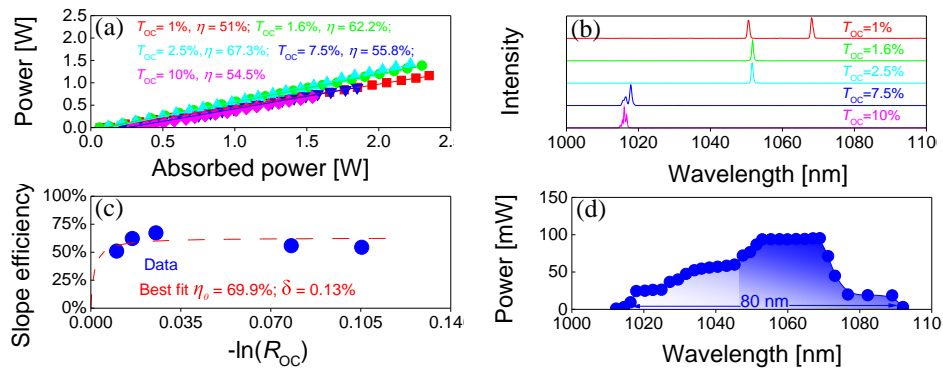


Fig. 2. (a) CW performance of the Yb:SALLO laser with different OCs, η – slope efficiency; (b) laser spectra; (c) Caird analysis: slope efficiency plotted as a function of the OC reflectivity ($R_{OC} = 1 - T_{OC}$); (d) spectral tuning curve obtained with an intracavity SF10 prism and an OC with $T_{OC} = 0.6\%$.

The total round-trip resonator losses δ (reabsorption losses excluded) as well as the intrinsic slope efficiency η_0 (accounting for the mode-matching efficiency and the quantum efficiency)

were estimated using the Caird analysis by fitting the laser slope efficiency as a function of the OC reflectivity ($R_{OC} = 1 - T_{OC}$) [21]. The best fitting curve gave $\eta_0 = 69.9\%$ and $\delta = 0.13\%$, as shown in Fig. 2(c). Such low value of δ is an evidence for the excellent optical quality of the Yb:SALLO crystal. The spectral tuning curve in the CW regime was studied at an absorbed pump power of 0.77 W using a SF10 prism and a 0.6% OC. The wavelength was continuously tunable between 1012 - 1092 nm corresponding to a range as broad as 80 nm, Fig. 2(d).

4. Mode-locked laser operation

Stable and self-starting SESAM ML operation was readily achieved by implementing two flat DMs ($DM_1 - DM_2$) into the cavity arm terminated by the OC, Fig. 1, which provided a total round-trip negative GDD of -2000 fs^2 to balance the material dispersion, as well as the induced self-phase modulation (SPM).

For 2.5% OC, the measured optical spectrum and the second harmonic generation (SHG) based intensity autocorrelation trace are shown in Fig. 3(a) and Fig. 3(b), respectively. The observed excellent sech^2 -shaped spectral and temporal profiles (although in theory in both cases this is an approximation) are an evidence for soliton-like pulse generation. The pulse duration of 94 fs at a central wavelength of 1054 nm and the emission bandwidth (FWHM) of 12.7 nm correspond to a time-bandwidth product (TBP) of 0.323 indicating nearly bandwidth-limited pulses. The inset of Fig. 3(b) shows an intensity autocorrelation trace on a longer time scale (50 ps) indicating single-pulse mode-locking without multiple pulse instabilities. The average output power of the ML laser amounted to 1.05 W for an absorbed pump power of 2.72 W. This corresponds to an optical efficiency of 38.6%. The recorded radio frequency (RF) spectrum of the laser output is shown in Fig. 3(c) and (d). A sharp peak at the fundamental beat note of 67.08 MHz exhibited a high extinction ratio of 76 dBc above the noise level. The uniform harmonics on a 1-GHz frequency span reveal high stability of the ML operation.

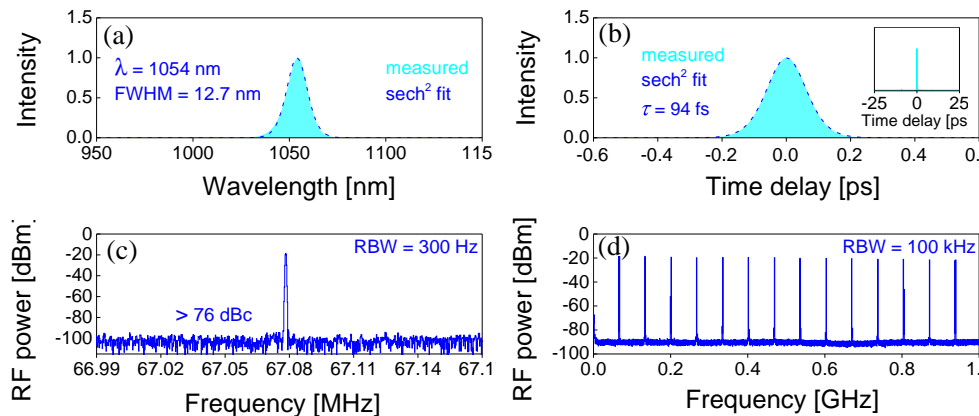


Fig. 3. SESAM ML Yb:SALLO laser with $T_{OC} = 2.5\%$. (a) Optical spectrum and (b) SHG-based intensity autocorrelation trace. *Inset* in (b): autocorrelation trace in a time span of 50 ps. RF spectra: (c) fundamental beat note at ~ 67 MHz recorded with a resolution bandwidth (RBW) of 300 Hz, and (d) harmonics on a 1-GHz frequency span, RBW = 100 kHz.

A rapid spectral broadening was observed by translating the folding mirror M_2 by few hundred of micrometers away from the laser crystal. After carefully aligning the cavity, the bandwidth (FWHM) of the laser spectrum increased from 12.7 to 22.6 nm, the average output power dropped to 404 mW and the central laser wavelength experienced a red-shift to 1062.8 nm, see Fig. 4(a).

The recorded autocorrelation trace gave a pulse duration of 53 fs (FWHM), as shown in Fig. 4(b). The corresponding TBP of 0.318 was even closer to the Fourier-transform limit. The long-time autocorrelation trace (Fig. 4(b), inset) and the RF spectra, Fig. 4(c-d), confirmed similarly stable and single pulse mode-locking performance.

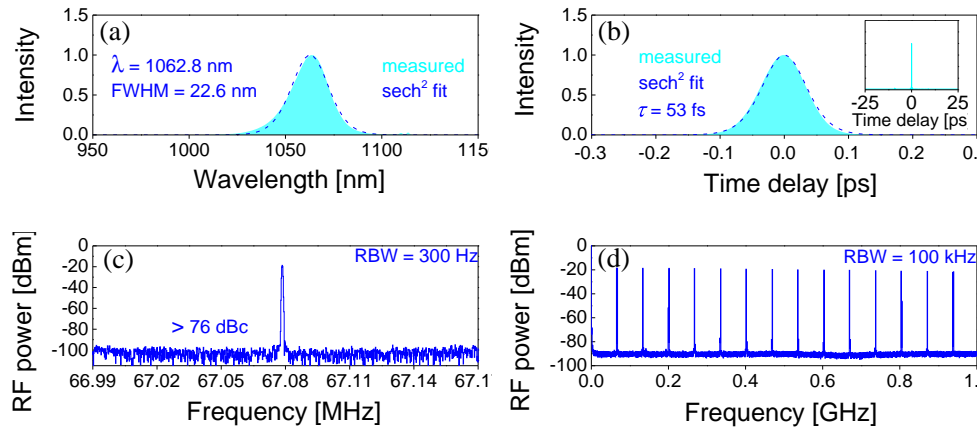


Fig. 4. KLM assisted SESAM ML Yb:SALLO laser with $T_{OC} = 2.5\%$. (a) Optical spectrum and (b) SHG-based intensity autocorrelation trace. Inset: autocorrelation trace on a time span of 50 ps. RF spectra: (c) fundamental beat note at ~ 67 MHz recorded with a resolution bandwidth (RBW) of 300 Hz, and (d) harmonics on a 1-GHz frequency span, RBW = 100 kHz.

Far-field beam profiles were measured to reveal the dominating ML mechanism for such a transition. An IR camera was placed ~ 1.1 m away from the OC. In the SESAM ML regime (cf. Figure 3), the laser beam diameters were $2.10 \text{ mm} \times 1.96 \text{ mm}$, see Fig. 5(a). After spectral broadening (cf. Figure 4), a significant change appeared in the measured far-field beam profile with a beam diameter of $1.89 \text{ mm} \times 1.89 \text{ mm}$, see Fig. 5(b). The shrinking of the far-field beam profile validated the underlying spectral broadening mechanism dominated by KLM stabilized by the SESAM, which is supported by the high brightness of the pump laser. Such soft-aperture Kerr-lens effect occurred due to the gradually increased laser mode size inside the Yb:SALLO crystal when varying the separation between the pump mirror M_1 and the folding mirror M_2 . Nevertheless, pulse shaping by the SESAM cannot be ruled out in view of the much wider stability zone and the self-starting mode-locking operation compared to our previous work [18]. Such hybrid pulse shaping mechanism introduced an enhanced self-amplitude modulation (SAM) by the Kerr-lens effect, which assisted the SESAM ML operation for shorter pulse duration, i.e., Kerr-lens assisted SESAM ML operation.

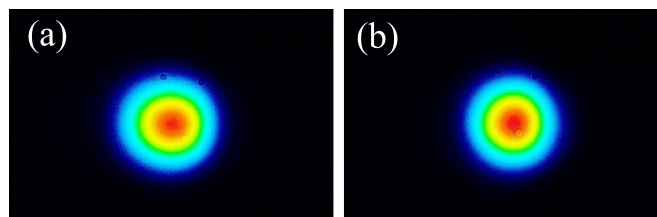


Fig. 5. Measured far-field beam profiles of the ML Yb:SALLO laser: transition of (a) SESAM ML to (b) Kerr-lens assisted SESAM ML regimes.

The pulse duration could be further shortened by reducing the total intracavity negative GDD in the Kerr-lens assisted SESAM ML regime. By implementing two extra bounces on flat DMs (DM₃ and DM₄, see Fig. 1) with a total negative intracavity GDD of -1620 fs^2 , the Yb:SALLO laser delivered soliton pulses as short as 38 fs at 1071 nm for the same 2.5% OC, see Fig. 6(a) and (b). The optical spectrum of the ML laser had a bandwidth (FWHM) of 32.2 nm assuming a sech^2 -shape spectral profile (due to the very strong SPM, the measured spectrum exhibited a slight deviation from such an ideal sech^2 -shaped spectral profile). The average output power amounted to 86 mW at an absorbed pump power of 0.78 W. The resulting TBP was 0.32, very close to the Fourier transform limit value (0.315). The steady-state ML pulse train corresponding to the shortest pulse duration was characterized by long scale autocorrelation, inset Fig. 6(b), and RF spectra, as shown in Fig. 6(c) and (d). The sharp first beat note at ~ 59.4 MHz with a signal-noise-ratio above 71 dBc, and the uniform harmonics again proved stable CW mode-locking without any Q-switched instability.

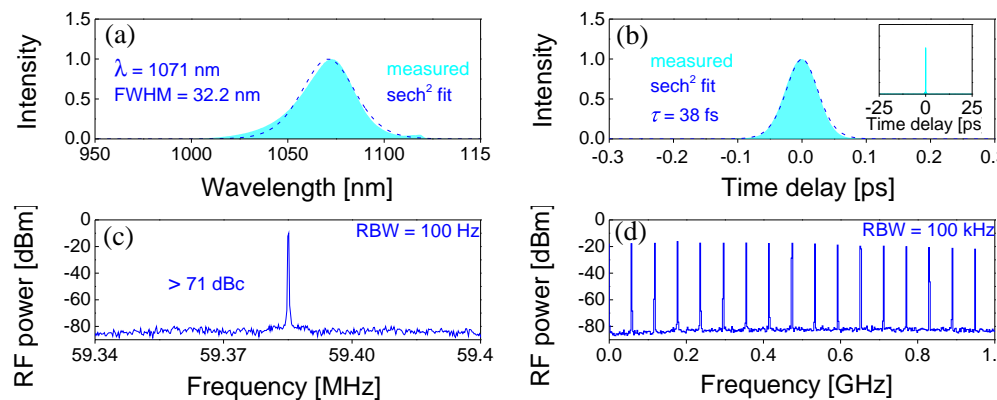


Fig. 6. Characterization of the shortest pulses from the ML Yb:SALLO laser. (a) Optical spectrum and (b) SHG-based intensity autocorrelation trace with a sech^2 -fit. *Inset:* simultaneously measured long-scale background free intensity autocorrelation trace for the time span of 50 ps. Radio-frequency (RF) spectra of the ML Yb:SALLO laser: (c) fundamental beat note at ~ 59.4 MHz recorded with a resolution bandwidth (RBW) of 100 Hz, and (d) harmonics on a 1-GHz frequency span, measured with a RBW of 100 kHz.

5. Conclusion

In conclusion, we demonstrate for the first time, to the best of our knowledge, SESAM ML operation of an Yb:SALLO laser. Assisted by enhanced self-amplitude modulation (SAM) originating from the Kerr-lens effect, the laser produced soliton pulses as short as 38 fs at 1071 nm with an average output power of 86 mW. Watt-level sub-100 fs pulse generation was obtained in the SESAM ML regime at the expense of longer pulse duration of 94 fs at 1054 nm: the average output power reached 1.05 W at an absorbed power of 2.72 W, which corresponded to a peak power of 146 kW and an optical efficiency of 38.6%. The excellent spectroscopic and thermo-mechanical properties of the Yb:SALLO crystal reveals a great potential for power scalable operation in the sub-50 fs time domain via Kerr-lens assisted SESAM ML technique in combination with commercially available high-power InGaAs pump diode lasers.

Funding. National Natural Science Foundation of China (61975208, 61875199, 51761135115, 61850410533, 62075090, 52072351); Sino-German Scientist Cooperation and Exchanges Mobility Program (M-0040); Foundation of President of China Academy of Engineering Physics (YZJLX2018005); Foundation of Key Laboratory of Optoelectronic

Materials Chemistry and Physics, Chinese Academy of Sciences (2008DP173016); Foundation of State Key Laboratory of Crystal Materials, Shandong University (KF2001).

Disclosures. The authors declare no conflicts of interest.

Data availability. Data underlying the results presented in this paper are not publicly available at this time but may be obtained from the authors upon reasonable request.

References

1. P. Loiko, J. M. Serres, X. Mateos, X. Xu, J. Xu, V. Jambunathan, P. Navratil, A. Lucianetti, T. Mocek, X. Zhang, U. Griebner, V. Petrov, M. Aguiló, F. Díaz, and A. Major, "Microchip Yb:CaLnAlO₄ lasers with up to 91% slope efficiency," *Opt. Lett.* **42**(13), 2431–2434 (2017).
2. P. Loiko, P. Becker, L. Bohatý, C. Liebold, M. Peltz, S. Vernay, D. Rytz, J. M. Serres, X. Mateos, Y. Wang, X. Xu, J. Xu, A. Major, A. Baranov, U. Griebner, and V. Petrov, "Sellmeier equations, group velocity dispersion, and thermo-optic dispersion formulas for CaLnAlO₄ (Ln = Y, Gd) laser host crystals," *Opt. Lett.* **42**(12), 2275–2278 (2017).
3. J. Yang, Z. Wang, J. Song, R. Lv, X. Wang, J. Zhu, and Z. Wei, "Diode-pumped 10 W femtosecond Yb:CALGO laser with high beam quality," *High Power Laser Sci. Eng.* **9**, e33 (2021).
4. W. Tian, Y. Peng, Z. Zhang, Z. Yu, J. Zhu, X. Xu, and Z. Wei, "Diode-pumped power scalable Kerr-lens mode-locked Yb:CYA laser," *Photonics Res.* **6**(2), 127–131 (2018).
5. P. Loiko, F. Druon, P. Georges, B. Viana, and K. Yumashev, "Thermo-optic characterization of Yb:CaGdAlO₄ laser crystal," *Opt. Mater. Express* **4**(11), 2241–2249 (2014).
6. P. Sévillano, P. Georges, F. Druon, D. Descamps, and E. Cormier, "32-fs Kerr-lens mode-locked Yb:CaGdAlO₄ oscillator optically pumped by a bright fiber laser," *Opt. Lett.* **39**(20), 6001–6004 (2014).
7. W. Tian, G. Wang, D. Zhang, J. Zhu, Z. Wang, X. Xu, J. Xu, and Z. Wei, "Sub-40-fs high-power Yb:CALYO laser pumped by single-mode fiber laser," *High Power Laser Sci. Eng.* **7**, e64 (2019).
8. S. Manjooran and A. Major, "Diode-pumped 45 fs Yb:CALGO laser oscillator with 1.7 MW of peak power," *Opt. Lett.* **43**(10), 2324–2327 (2018).
9. W. Tian, R. Xu, L. Zheng, X. Tian, D. Zhang, X. Xu, J. Zhu, J. Xu, and Z. Wei, "10-W-scale Kerr-lens mode-locked Yb:CALYO laser with sub-100-fs pulses," *Opt. Lett.* **46**(6), 1297–1300 (2021).
10. N. Modsching, C. Paradis, F. Labaye, M. Gaponenko, I. J. Graumann, A. Diebold, F. Emaury, V. J. Wittwer, and T. Südmeyer, "Kerr lens mode-locked Yb:CALGO thin-disk laser," *Opt. Lett.* **43**(4), 879–882 (2018).
11. W. Tian, C. Yu, J. Zhu, D. Zhang, Z. Wei, X. Xu, and J. Xu, "Diode-pumped high-power sub-100 fs Kerr-lens mode-locked Yb:CaYAlO₄ laser with 1.85 MW peak power," *Opt. Express* **27**(15), 21448–21454 (2019).
12. A. Greborio, A. Guandalini, and J. Aus der Au, "Sub-100 fs pulses with 12.5-W from Yb:CALGO based oscillators," *Proc. SPIE* **8235**, 823511–823516 (2012).
13. Y. Wang, X. Su, Y. Xie, F. Gao, S. Kumar, Q. Wang, C. Liu, B. Zhang, B. Zhang, and J. He, "17.8 fs broadband Kerr-lens mode-locked Yb:CALGO oscillator," *Opt. Lett.* **46**(8), 1892–1895 (2021).
14. J. Ma, F. Yang, W. Gao, X. Xiaodong, X. Jun, D. Shen, and D. Tang, "Sub-five-optical-cycle pulse generation from a Kerr-lens mode-locked Yb:CaYAlO₄ laser," *Opt. Lett.* **46**(10), 2328–2331 (2021).
15. F. Labaye, V. J. Wittwer, M. Hamrouni, N. Modsching, E. Cormier, and T. Südmeyer, "Yb-doped laser oscillator generating 22-fs pulses at 0.73 W," in *Conference on Lasers and Electro-Optics, OSA Technical Digest* (Optical Society of America, 2021), paper SF2M.5.
16. S. Kimura, S. Tani, and Y. Kobayashi, "Raman-assisted broadband mode-locked laser," *Sci. Rep.* **9**(1), 3738 (2019).
17. Z. B. Pan, X. J. Dai, Y. H. Lei, H. Q. Cai, J. M. Serres, M. Aguiló, F. Díaz, J. Ma, D. Y. Tang, E. Vilejshikova, U. Griebner, V. Petrov, P. Loiko, and X. Mateos, "Crystal growth and properties of the disordered crystal Yb:SrLaAlO₄: a promising candidate for high-power ultrashort pulse lasers," *CrystEngComm* **20**(24), 3388–3395 (2018).
18. Z. L. Lin, H. J. Zeng, G. Zhang, W. Z. Xue, Z. Pan, H. Lin, P. Loiko, H. C. Liang, X. Mateos, V. Petrov, L. Wang, and W. Chen, "Kerr-lens mode-locked Yb:SrLaAlO₄," *Opt. Express* **29**(26), 42837–42843 (2021).
19. A. Pajczkowska, A. V. Novosselov, and G. V. Zimina, "On the dissociation and growth of SrLaGaO₄ and SrLaAlO₄ single crystals," *J. Cryst. Growth* **223**(1-2), 169–174 (2001).
20. W. Ryba-Romanowski, S. Gołab, I. Sokolska, W. Pisarski, G. Dominiak-Dzik, A. Pajczkowska, and M. Berkowski, "Anisotropy of optical properties of SrLaAlO₄ and SrLaAlO₄:Nd," *J. Alloy. Compd.* **217**(2), 263–267 (1995).
21. J. A. Caird, S. A. Payne, P. R. Staver, A. Ramponi, and L. Chase, "Quantum electronic properties of the Na₃Ga₂Li₃F₁₂:Cr³⁺ laser," *IEEE J. Quantum Electron.* **24**(6), 1077–1099 (1988).